

Non-Unity Active PFC Methods for Filter Size Optimization

Y. Chen J. W. Kimball P. T. Krein
Grainger Center for Electric Machinery and Electromechanics
Department of Electrical and Computer Engineering
University of Illinois, Urbana, Illinois 61801 USA

Abstract – Active power factor correction seeks to obtain unity power factor and sinusoidal line currents. Optimized non-sinusoidal line currents reduce filter capacitor requirements with a non-unity target power factor. Implementation methods are presented that permit reduced power factor to be traded off against filter size in a nearly optimum manner. A simple waveform shape can reduce filter component size by about 40% in active PFC converters at the same level of complexity as in conventional PFC designs while yielding power factor as high as 0.9. Two approximate methods to generate appropriate shapes are presented. They offer direct practical implementation of non-unity power factor solutions and have been verified experimentally. Such solutions meet power quality standards and deliver acceptable power factor with reduced converter cost.

I. INTRODUCTION

Active power factor correction (PFC) is a topic of wide interest. Active PFC designs in general seek to achieve unity power factor and exhibit very low harmonic distortion. As pointed out in [1], the all-or-nothing ideal unity power factor approach goes well beyond requirements of power quality standards. Worst-case waveforms within the allowed range of IEC 61000-3-4 [2] and other standards, for example, have very poor power factor indeed. Designs based more directly on the standards are being discussed [3]-[4]. A valid argument is that such standards have been written to “tolerate” nonlinear load currents such as those from rectifiers, but in any case power system engineers do not design for unity power factor. Therefore, a designer would naturally ask whether non-unity power factor can be used to advantage in a power converter design. For example, can a power factor such as 0.9 or 0.85 (which would be considered quite acceptable for a linear load) be specified in exchange for reduced cost?

Ref. [5] sets up the non-unity power factor problem, and shows that there are *optimum* current waveform choices for given values of power factor. This choice of optimum waveform minimizes power ripple at the output of the switching converter for a given power factor. Reducing power ripple then minimizes the size of the filter capacitor required in an active PFC power converter. The waveforms identified in the optimization process in [5] do not resemble those of an uncontrolled rectifier. The optimal waveforms are not achieved by starting with a unity power factor circuit and just reducing filter size or loop gain. Rather, the waveforms involve specific harmonic components. Two drawbacks of [5] were as follows:

- The study was purely simulated and implementation complexities were ignored.

- There was no exploration of whether convenient approximations to the optimum waveforms could offer any benefits.

This paper revisits the non-unity power factor scheme introduced in [5] to explore how the technique can be made practical, and how it might contribute to actual commercial designs of power converters. Does non-unity power factor save enough to be useful? Approximate waveforms are shown to yield nearly the same benefits as the optimum ones if the shapes are chosen properly. Two practical implementations are identified, each easier than the harmonic waveforms in [5], that yield only a few percent larger filter capacitance than the optimum.

Operating experimental results are provided that confirm the speculation in [1] that non-unity power factor can be used in the design process to advantage. The results also support a waveform identified in [4]. The implementation complexity of the second proposed method is nearly identical to that of conventional gain-controlled active PFC control loops. For essentially the same control cost, power converter cost can be reduced substantially by using non-unity power factor. A specific target power factor can be chosen during the design (or even set as an adjustment in the control loop) to meet customer needs while performing acceptably with respect to the input power system. Typically, the capacitor required for filtering can be reduced by at least 40% when reasonable power factors are selected.

II. OPTIMUM DOUBLE-FREQUENCY POWER MANAGEMENT

A fundamental issue in any single-phase conversion application is the double-frequency power term. In a single-phase active PFC power supply application, ideal current is drawn from the input supply, but the output is a fixed dc potential. The input instantaneous power from the supply carries a large double-frequency term while the output power is constant. The double-frequency term must be managed within the converter and the filter components carry it at full strength. The line-side power factor is unity. In principle, the opposite extreme is also possible. In this case, the converter acts to draw near-fixed power during dynamic operation. The double-frequency power is forced to flow in the source, and the filter only addresses switching frequency components. The line-side power factor is low – about 0.12 in a near-ideal case [5] – reflecting the fact that high reactive power flows are being demanded to cover the double-frequency power term internally within the source.

In terms of filter design practice, the two extremes – unity power factor compared to constant power – are vastly different.

Unity power factor requires thousands of microfarads, and it is usually helpful to buffer the converter with a second stage. Constant power minimizes filter size at the expense of much higher component and input supply losses. The extremes do not optimize trade-offs between filter size and loss. In contrast, results in [5] identify an optimum trade-off between double-frequency power handling within the converter and within the input supply. For any given power factor there is a specific current to use. For example, a target power factor of 0.9 and line voltage $v(t) = V_0 \cos(\omega t)$ yield the optimum current waveform

$$i(t) = I_0 [\cos(\omega t) - 0.433 \cos(3\omega t) + 0.216 \cos(5\omega t)] \quad (1)$$

Here I_0 is a scaling factor set to deliver the correct average power. Other specified power factors yield different currents, although certain relationships remain unchanged: the last harmonic is $-1/2$ times the second last, etc. Over a substantial power factor range (about 0.88 to almost 1), the third harmonic amplitude in (1) represents a single degree of freedom to be adjusted for optimum filter size. For power factor in the range of 0.8 to 0.88, seventh harmonic is added. Again, the choice of waveform can be reduced to a single degree of freedom. The optimum waveform to achieve 80% power factor with seventh harmonic added is

$$i(t) = I_0 \left[\begin{array}{l} \cos(\omega t) - 0.601 \cos(3\omega t) \\ + 0.401 \cos(5\omega t) - 0.2 \cos(7\omega t) \end{array} \right] \quad (2)$$

While these waveforms provide the best results, they are not easy to generate.

III. IMPLEMENTATION AND RESULTS

A. Structure and the Need for Approximate Waveforms

Consider a boost active rectifier stage, as conventionally used for active PFC. Fig. 1 shows an example converter that was used to experimentally verify the techniques. In principle, the expressions in (1) or (2) can be used to define a reference current. This can be phase-locked to the incoming ac voltage, then treated in a manner similar to the sinusoidal current reference that is used in a conventional active PFC converter. However, the harmonic terms in (1) and (2) may require separate oscillators and phase locking methods may be more complicated than necessary in this application.

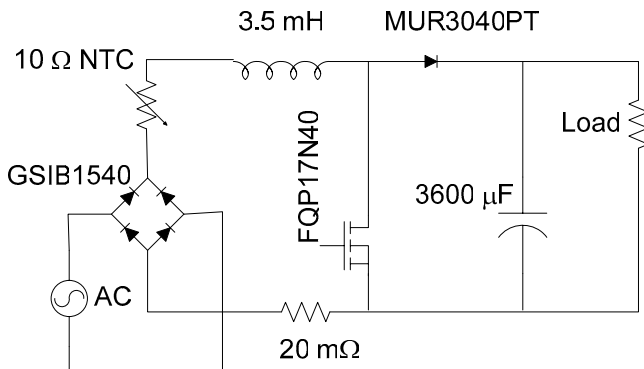


Fig. 1. Boost converter for active PFC (experimental values shown).

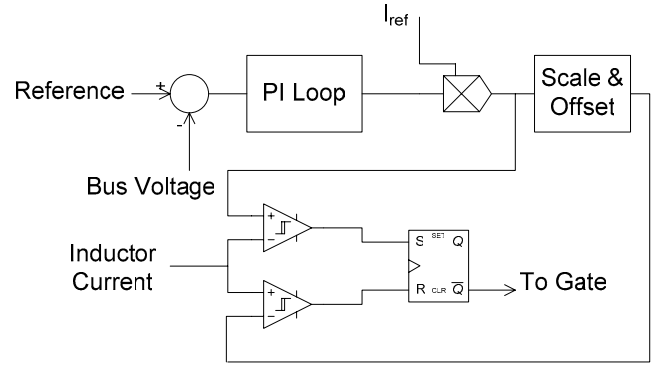


Fig. 2. Typical hysteretic current controller used for PFC.

There is a need to seek a less complicated alternative to the harmonic waveforms of (1) and (2). If a waveform can be generated from a simplified procedure – ideally directly from the voltage waveform – it can take the place of a sinusoidal waveform and provide the size reduction benefits of reduced power ripple while meeting power factor constraints. Any such approximate waveform will be sub-optimal, but it is worth exploration to see how close an approximation can come. In this section, two alternative approaches are discussed to provide approximate current waveforms. Neither requires computation of harmonics. The circuits discussed generate I_{ref} , a reference waveform, as an input to a standard hysteretic controller such as that shown in Fig. 2.

B. Partial Constant Power Waveform Approximation

The first approach uses a current waveform that draws constant power from the source over a portion of each cycle. Over the half-cycle angle interval from $-\pi/2$ to $\pi/2$, the waveform is defined as

$$i(t) = I_0 \begin{cases} \frac{\cos^2(\omega\alpha)}{\cos(\omega t)}, & -\alpha < \omega t < \alpha \\ \cos(\omega t), & \text{otherwise} \end{cases} \quad (3)$$

This has the effect of constant power over the interval from $-\alpha$ to α . For this current, the power from the source $p(t) = i(t)V_0 \cos(\omega t)$ is

$$p(t) = V_0 I_0 \begin{cases} \cos^2(\omega\alpha), & -\alpha < \omega t < \alpha \\ \cos^2(\omega t), & \text{otherwise} \end{cases} \quad (4)$$

These current and power waveforms for a sample value of α are shown in Figs. 3 and 4, respectively, and are compared there to the optimum waveforms based on a target power factor of 80%, as in (2).

The value of α provides a single degree of freedom to set a desired power factor. Given α , the power factor can be computed as

$$\text{pf}(\alpha) = \frac{P_{in}}{V_{rms} I_{rms}} = \frac{\pi + \alpha \cos(2\alpha) - \sin(2\alpha)}{\sqrt{\pi^2 + \pi \sin(2\alpha) - 2\pi\alpha}} \quad (5)$$

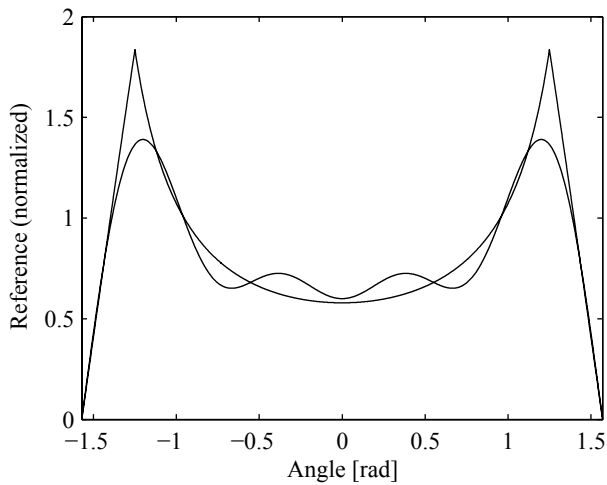


Fig. 3. Half-cycle current from (3) compared to optimum current (2) for 80% power factor. The optimum exhibits obvious harmonics.

Table 1 compares the relative filter capacitor sizes based on the optimum power waveform and approximate power waveform in Fig. 4. The values are normalized to the unity power factor case. The approximate waveform requires 3-5% more capacitance than the optimum case for a given target power factor. Notice that a target power factor of 85% reduces the filter capacitor size by about 40% relative to the unity power factor solution.

TABLE I. CAPACITANCE VALUES FOR PARTIAL CONSTANT POWER APPROXIMATION.

Power factor	Optimum capacitance, normalized to pf=1, from [5].	Approximate waveform result
0.80	0.529	0.535
0.85	0.579	0.594
0.90	0.644	0.669
0.95	0.736	0.765

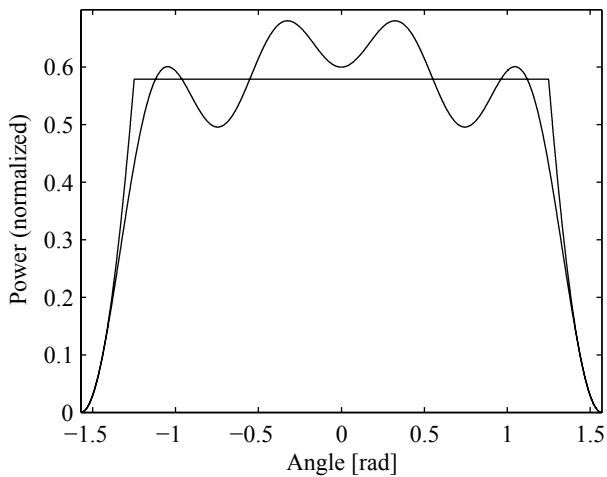


Fig. 4. Power half-cycle waveforms based on current in (2) and power in (4) for target power factor of 80%. The approximate result in (4) yields the flat-top waveform.

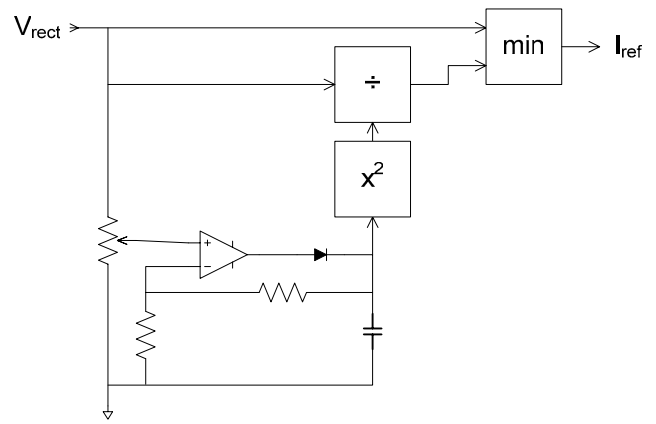


Fig. 5. Partial constant power approximation circuit.

The partially constant power approximation method has been implemented in hardware and tested experimentally. The current waveform was generated with an analog circuit from the voltage, then used as the reference in a conventional current-hysteresis active PFC boost converter (Figs. 1 and 2). A block diagram of the circuit is shown in Fig. 5. The square and divide blocks are implemented with analog multipliers. The minimum function is implemented with window comparators. The line input waveforms are given in Fig. 6, based on target power factor of 0.8.

The approximation in (3) yields a continuum of solutions between unity power factor and constant power. Since the angle α defines the constant power time interval, it is straightforward to see how reduced power ripple during a portion of the cycle can be traded off against power factor. Circuitry to implement (3) is complicated. In particular, the analog divider in Fig. 5 is sensitive to component specifications as well as to layout details.

C. Partial Inverted Waveform Approximation

A second approximate method is suggested by the geometry of the approximate current waveform in Fig. 3. The

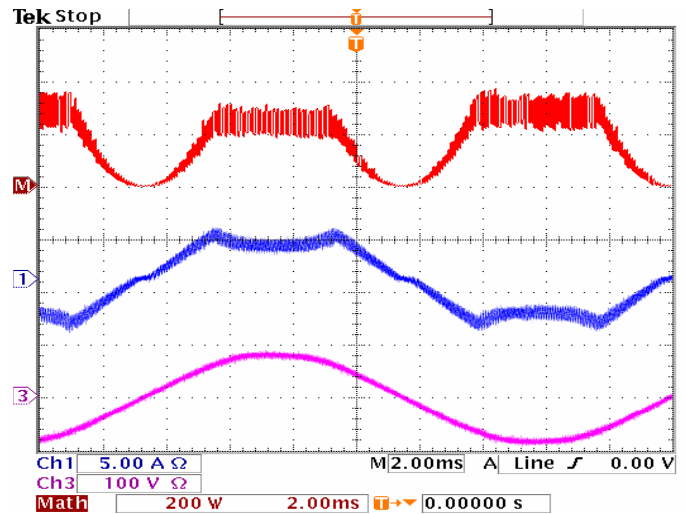


Fig. 6. Power (top trace), line current, and line voltage for partial constant power approximation.

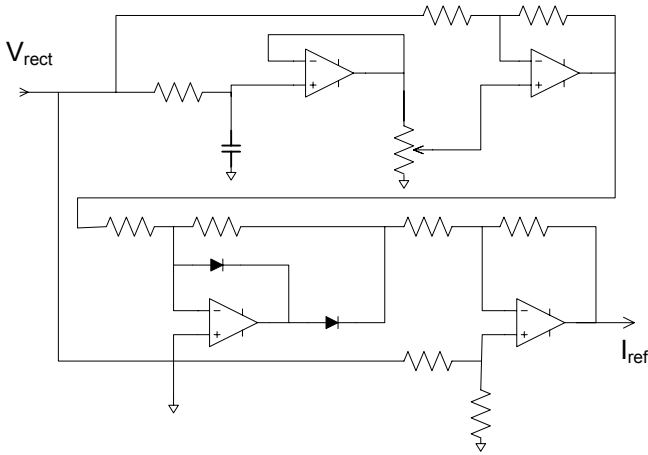


Fig. 7. Circuit to construct (6).

waveform looks as if it is inverted over the interval $[-\alpha, \alpha]$. Over the half cycle from $-\pi/2$ to $\pi/2$, this effect can be written

$$i(t) = I_0 \begin{cases} \cos(\omega t) - k[\cos(\omega t) - \cos(\alpha)], & -\alpha < \omega t < \alpha \\ \cos(\omega t), & \text{otherwise} \end{cases} \quad (6)$$

There are two degrees of freedom in k and α , which makes it less clear how to select a waveform. However, it has been determined that results do not vary much with k . The choice $k = 1.25$ yields excellent performance. Thus the result can be reduced to a single degree of freedom α that sets the target power factor.

The waveform of (6) can be generated with op-amps based on fixed gains, truncation, and subtraction, as shown in Fig. 7. The resulting power $p(t) = i(t)V_0\cos(\omega t)$ is

$$p(t) = V_0 I_0 \begin{cases} \cos^2(\omega t)(1-k) + k \cos(\omega t) \cos \alpha, & -\alpha < \omega t < \alpha \\ \cos^2(\omega t), & \text{otherwise} \end{cases} \quad (7)$$

Sample current and power half-cycle waveforms are given in Figs. 8 and 9, respectively. Let $\xi = \sin(2\alpha)$. The power factor, based on (7), can then be written as

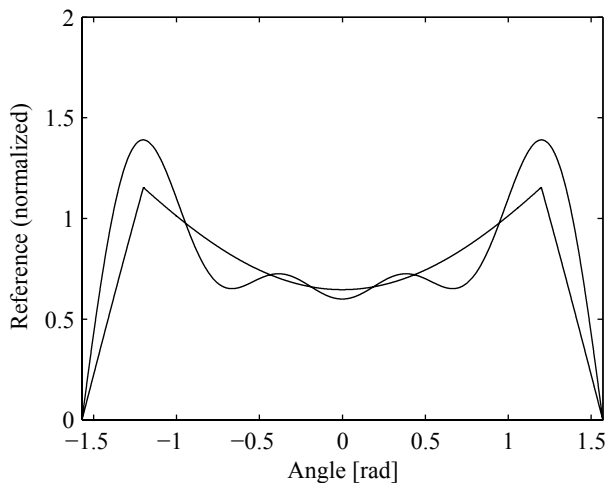


Fig. 8. Half-cycle current from (6) compared to optimum current (2) for 80% power factor. The optimum exhibits obvious harmonics.

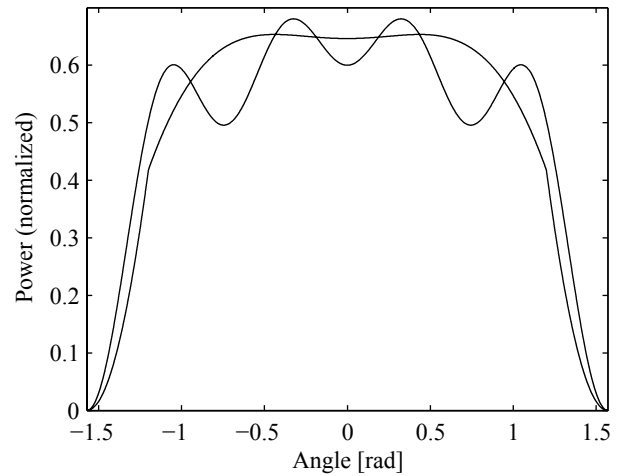


Fig. 9. Power half-cycle waveforms based on current in (2) and power in (7) for target power factor of 80%. The approximate result in (7) yields the nearly-flat-top waveform.

$$\text{pf}(\alpha) = \frac{\pi + k\xi - 2k\alpha}{\sqrt{\pi^2 + 4k^2\pi\alpha\cos^2\alpha - 3k^2\pi\xi + 2k\pi\xi + 2k^2\pi\alpha - 4k\pi\alpha}} \quad (8)$$

This approach yields capacitance requirements within 2% of those produced by the optimum waveform.

Experimental waveforms have been obtained. Fig. 10 shows power, source voltage, and line current traces for the partial inverted waveform method. The resulting power factor is 86%.

The implementation of the partial inverted waveform method is simple, and (6) offers the promise of direct replacement for the sinusoidal waveform in a conventional unity power factor design. The overall complexity is essentially the same as for a conventional unity PFC

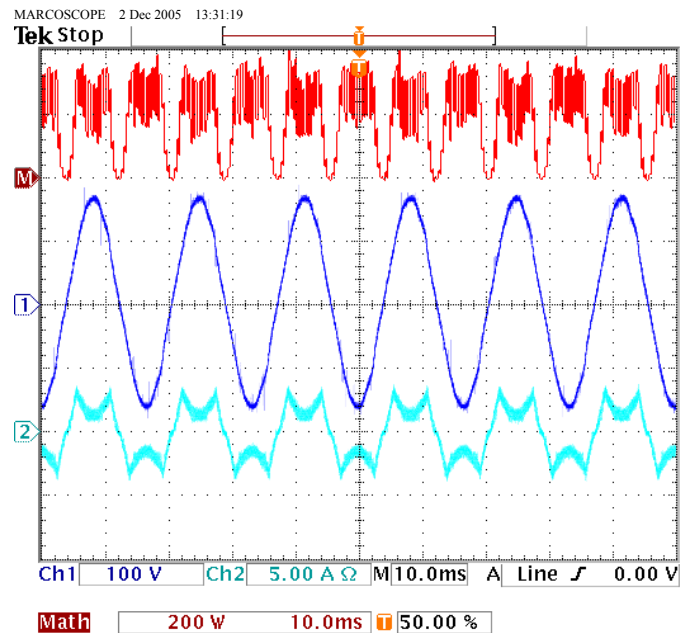


Fig. 10. Power (top trace), line voltage (center trace), and line current (bottom trace) for partial inverted waveform method with a target power factor of 90%

application. This means that truncation and subtraction steps can be used to reduce filter capacitance by about 40% (for the choice $pf = 0.85$) with an otherwise conventional active PFC circuit. Resulting bus voltage waveforms are shown in Fig. 11 for unity power factor and $pf = 0.86$ with the partial inverted waveform approximation. The rms voltage ripple decreases by 41% for the reduced power factor control, as expected.

IV. CONCLUSION

Non-unity power factor methods allow filter size reduction in active PFC converters. The optimum current waveform to minimize filter size for a given choice of power factor is known [5], but the results there involve specific harmonic-based waveforms and are hard to implement. This paper has shown two approximate methods that deliver near-optimum filter size based on waveforms that can be developed from the input voltage sinusoid. The approximate methods deliver results within a few percent of the optimum. A designer can now choose to deliberately set a non-unity power factor in exchange for filter size and cost reduction. The reduction is substantial – about a 40% decrease in main filter capacitor size for a selected power factor of 85%.

The results apply to all PFC converter methods [6] but match particularly well to low-cost converters. The extra cost of a switching converter can now be traded off against filter component cost and the indirect costs of low power factor. The methods described here provide convenient, practical ways to implement optimized non-unity power factor solutions.

REFERENCES

[1] O. Garcia, J. A. Cobos, R. Prieto, P. Alou, J. Uceda, "Single phase power factor correction: a survey," *IEEE Trans. Power Electronics*, vol. 18, no. 3, pp. 749-755, May 2004.

[2] International Electrotechnical Commission, standard IEC 61000, "Electromagnetic compatibility (EMC) - Part 3-4: Limits - Limitation of emission of harmonic currents in low-voltage power supply systems for equipment with rated current greater than 16 A."

[3] A. Fernandez, J. Sebastian, M. Hernando, P. Villegas, J. Garcia, "Helpful hints to select a power-factor-correction solution for low- and medium-power single-phase power supplies," *IEEE Trans. Industrial Electronics*, vol. 52, no. 1, pp. 46-55, February 2005.

[4] A. Lazaro, A. Barrado, J. Pleite, E. Olias, "New power factor correction ac/dc converter with reduced storage capacitor voltage," in *Proc. IECON*, 2002, pp. 353-358.

[5] P. T. Krein, "Current quality and performance tradeoffs under active power factor correction," in *Proc. IEEE Workshop Computers in Power Electronics (COMPEL)*, 2004, pp. 97-101.

[6] C. K. Tse, M. Chow, "A theoretical examination of the circuit requirements of power factor correction," in *Rec. IEEE Power Electronics Specialists Conf.*, 1998, pp. 1415-1421.

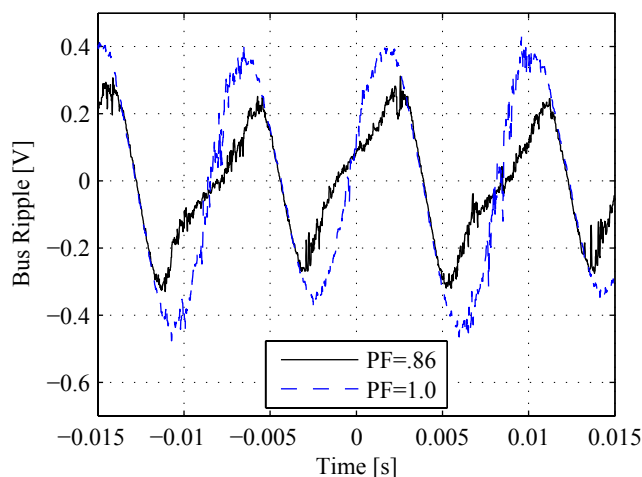


Fig. 11. Bus voltage ripple (ac coupled) for unity power factor and for partial inverted waveform with reduced power factor of 0.86.